Technological-economic study of a unique hydrogen-based hybrid energy system for on-grid and off-grid use: Tegal-Pesawaran-Lampung Islands, Indonesia

Iwan Purwanto[1*], *Dikpride* Despa [2], and *Aleksander* Purba [2]

[1] Student of Engineering Professional Program, Faculty of Engineering, Lampung University
[2] Engineering Professional Program, Faculty of Engineering, Lampung University

Abstract. Indonesia has several uninhabited islands. Lack of basic facilities like a place to eat may hinder corporate value-raising. Indonesia has unique energy issues as a developing country, but integrating new energy sources to fulfill regional demands is a viable option. This article describes a cutting-edge hydrogen-based hybrid energy system (HRES) that produces hydrogen fuel from solar-powered electrolysis and supercritical water gasification (SCWG). It is commonly known that hydrogen can store freshly generated energy until heat is introduced to turn it into electricity via fuel source pyrolysis. In typical residential areas of Pulau Tegal, Pesawaran-Lampung, the HRES provides base load energy. Technology and economic evaluation of the designed system uses an integrated optimization and simulation framework to minimize total system costs while operating off-grid and maximize profits from using cutting-edge electricity generation methods and selling excess power to the grid. The planned HRES can produce 47,3 MWh of energy under all scenarios, which is enough to meet the area's external demand during the study. Scenario 1 has a 55,92 IDR/kWh levelized energy cost (LCOE), whereas Scenario 2 has 56,47 IDR/kWh.

1. Introduction

Indonesia is an out-of-the-ordinary island nation. Indonesia, which is situated in South East Asia, is made up of more than 17,0 islands, making it the country with the highest number of islands in the world. About 6,000 of these islands are inhabited during the day [1]. Due to the country's many islands, Indonesian culture, language, and customs are very diverse. Each island and province in Indonesia has its own distinct culture, traditions, and cultural artifacts. As a nation of islands, Indonesia has challenges in natural resource management, inter-island connectivity, and transportation. The root of the problem is the absence of a central registry on that island. This phenomenon has become rather intriguing, and scholars have been working hard to uncover its secrets and explain them.

* Corresponding author: iwan.purwanto@trisakti.ac.id

Indonesia's government may alleviate this problem by expanding the country's energy infrastructure to include more modern energy sources. Assessing the environmental effects of increasing fossil fuel use and taking steps to mitigate such effects [1]. Because all renewable energy is dependent on water, it is expensive to develop a reliable power infrastructure. We will provide continuous, low-cost electricity from a combination of renewable energy sources (RER), including existing power plants and newer technologies like solar photovoltaic and wind turbines. A cutting-edge hybrid energy system (HRES) coupled to a storage device like a battery or hydride tank can store and utilize renewable energy sources like the sun and wind even when traditional power sources are unavailable. Thus, HRES outperforms a single cutting-edge technology in all weather circumstances, emphasizing the importance of energy saving in specialized power systems.

Despite being the most promising energy storage technology, batteries have a limited useable life, low efficiency, and environmental impacts from incorrect disposal. Hydrogen, which has a far larger storage capacity than batteries, may be utilized to backup energy in an HRES configuration. Hydrogen may be utilized to generate power and heat space, lowering HRES's leveling cost of energy (LCOE). The manufacturer may produce hydrogen using solar-powered electricity generation, thermal-energy recovery systems, biomass gasification, or metabolic processes like biochemical fermentation, depending on the hydrogen-based HRES design.

Conventional biomass gasification is the most promising for HRES hydrogen production [2, 3]. However, pre-combustion and post-combustion processes must be taken into account in this approach in order to increase efficiency in hydrogen production. One recent development in hydrogen production is the use of air as a gasification agent at temperatures and pressures above its critical point (374 degrees Celsius and 22.1 mega parcels). Significant improvements in overall gasification and hydrogen production have been shown using supercritical water gasification (SCWG) [4, 5]. SCWG produces carbon monoxide-methane syngas, which may be burnt in supplementary boilers to heat the process to 650 C. SCWGs burn biomass feedstock without pretreatment. [4].

Academics worldwide are studying hydrogen-based HRES technology analysis. Analytical methods for hydrogen-based HRES design have been presented in recent works. Discusses the economics of biomass fermentation using HRES, which includes PV modules, wind turbines, an electrolyser, and biomass fuel stock. [6]. The system may operate as a stand-alone Bio-HRES, generating 31 MWh of electrical power, hot water, and hydrogen for an LCOE of $0.793 per kilowatt-hour. Utilizing PSO) [7–10]. Discuss the best design for hydrogen-based HRES in order to minimize overall system costs and carbon dioxide emissions. Their system consists of a solar-powered battery bank, a diesel generator, an electric turbine, and a supply of cooked rice. The estimated 25-year lifetime cost of the system is EUR 93,487. Table 1 displays the scope of recent hydrogen-based HRES research using several approaches to modelling the economy. Review table of setup and modelling methodologies for hydrogen-based hybrid renewable energy systems (HRES).

Table 1: scope of recent hydrogen-based HRES research using several approaches to modelling the economy

System Components								Objective Function	Method	Ref
WT	PV	FC	Biomass	Battery	H2 TNK	Electrolyser	Diesel Other			
√	√	√		√	√	√	√	Value Added/Carbon Emissions/ Unmet Demand	PSO [1]	[11]

√	√	√		√	√	√	√	Σ cost	SA [2]	[12]
√	√	√		√	√	√	√	Σ cost /CO_2 Emission/ excess demand	GA [3]	[13]
√	√	√			√	√	√	Σ cost /CO_2 Emissions/unmet bad	FL [4]	[14]
√		√	√	√	√			LCOE	LP [5]	[15]
√	√	√	√	√	√			Cost per year	GA	[16]
√	√	√		√	√	√	√	Overall cost	GA	[17]

*) [1]Particle swarm optimization; [2] simulated annealing; [3] genetic algorithm; [4] fuzzy logic; [5] linear programming

The scientific community has paid considerable attention to the prospect of combining biomass gasification with hybrid systems. All of these studies concentrate on combining a hybrid system of solid fuel gasification with combustion [4, 5].The SCWG and bacon fat combination is a novel idea. However, prior research on SCWG reintegrated raw materials is lacking, and this study seeks to fill that gap.

This plan combines solar thermal water generation (SCWG) and solar thermal power generation (STEP) to create an efficient hydrogen-based HRES. HRES electricity comes from solar panels and a biomass boiler. The electrolyser decomposes air to make hydrogen using extra solar electricity. Hydrogen tanks store it thereafter. A system of roasted coconut cadenzas may create hydrogen-based power without sunshine. Supercritical water gasification (SCWG) uses supercritical air to create hydrogen to mitigate hydrogen shortages in hydropower networks. SCWG uses domestic food with a 40% water content.

Hydrogen stores freshly produced energy until heat transforms it to electricity, according to this research. A solar thermal power plant or a combined heat and power (CHP) plant that hydrothermally converts biomass into hydrogen may produce hydrogen. Supercritical water gasification (SCWG) transforms organic biomass like wood chips and grass clippings into hydrogen, carbon dioxide, carbon monoxide, and methane. SCWG also addresses several biomass gasification difficulties. Electrolysis of water produces hydrogen and is ecologically favorable. Electrolysis of alkaline water to make hydrogen from solar energy is the most promising method for clean, efficient renewable energy production. The sole byproduct is oxygen, which does not emit carbon. Proton-exchange membrane (PEM) fuel cells are also being studied because to their smaller size, higher efficiency, quicker reaction times, lower working temperatures (20-80 degrees Celsius), and appropriateness for residential applications.

In rural parts of Tegal Island Prefecture, Indonesia, the suggested system will minimize power demand and supply. HRES can boost renewable energy generation and tree management in the selected residential area. Figure 1 shows the HRES setup.

Technological analysis and the integrated modelling and simulation framework will be used to design HRES optimally outside of economic optimality. This model analyzes the level-zed cost of energy (LCOE) sensitivity to two scenarios. (2) a grid-connected, FiT-based system.

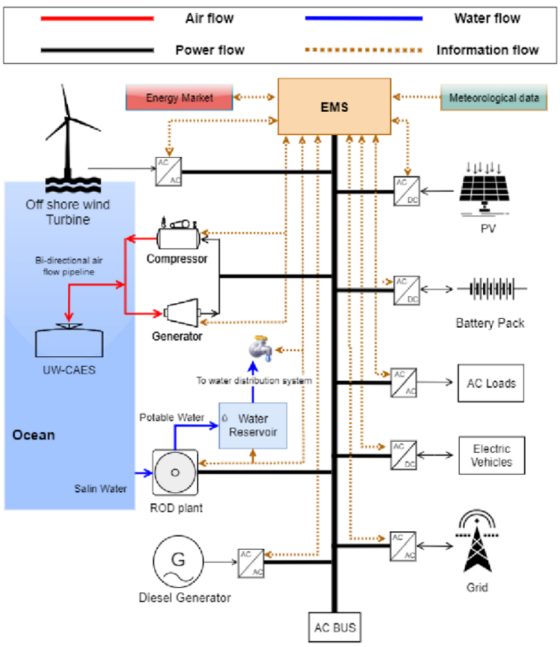

Figure 1. Proposed system configuration

2. Simulation Model

2.1. PV Panel

The following equations may be used to determine the PV array's output power [18]:

$$P_{PV} = P_{max} P_{PV} \left(\frac{\overline{I_T}}{G_{T,STC}}\right)\left[1 + \propto_p \left(T_c - T_{c,STC}\right)\right] \quad (1)$$

$$T_c = T_a + G_T \left(\frac{T_{c,NOCT} - T_{a,NOCT}}{G_{T,NOCT}}\right)\left(1 - \frac{n_{cell}}{\tau\alpha}\right) \quad (2)$$

Pmax is the maximum PV panel output in kilowatts; F_{PV} is a PV de-rating factor that relies on PV module characteristics like clarity (%). IT and GT,STC are normal radiation levels. T_c is the lowest modulus of photovoltaic cells; Ta is the temperature range around NOCT (nominal operating cell temperature); and cell is the highest efficiency of a solar cell at that temperature. PV cell temperatures are $T_{c,STC}$ and T_a. NOCT is maximum power point efficiency at operational temperature. Table 2 lists the key input data for Equations (1) and (2).

Table 2. Primary input data used for PV output estimation

Parameter	Symbol	Value
Coefficient of temperature (%/deg)	αp	−0.258
Optimal performance	ηmax	0.217
Rated output (W)	P_{max}	325
Cell operating temperature nominal (°C)	$T_{c,\ NOCT}$	44

Typical working environment temperature (°C)	$T_{a,\ NOCT}$	20
Radiation dose under experimental conditions (W/m^2)	$G_{T,STC}$	1000
Ratings reduction	FPV	0.9
Thermodynamic conditions in the test cell (°C)	$T_{C,STC}$	25

The connection between the sun's rays and the solar panels is seen in Figure 2.

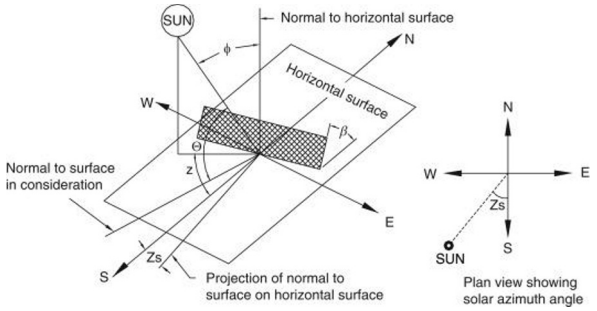

Figure 2. Connections between the Sun's rays and solar panels.

The radiation that reaches the PV surface is a function of the local environment, the passage of time, and the epoch of the Earth's revolution, all of which may be estimated using the formulas provided below [19]:

$$I_T = I_{grobal}\left\{\left(\cos\psi\cos k + \sin\psi\sin k\cos(\lambda-\zeta) + \mu\cos\frac{\psi}{2}\right) + \rho\left(\cos k + \mu\sin^2\frac{\psi}{2}\right)\right\} \quad (3)$$

where Ignoble is the global radiation at the surface perpendicular to the sunlight vector (kW/m^2); ψ is the angle of inclination between the photovoltaic panels and the ground, which is parallel to the horizon; ψ is a ground-dependent reflection index; and represent the sun's azimuth on the celestial sphere and the plates' azimuth angles (eastern radian larger than 0 and western radiation less than 0). The solar zenith angle (κ) is the sun's beams' angle with the horizontal plane.

$$\cos\kappa = \sin\delta\sin\gamma + \cos\delta\cos\gamma\cos\alpha \quad (4)$$

where γ is the measured latitude and δ is the sun's celestial sphere declination angle, relating to its height. The angle between the line connecting the sun's centre to the earth and its projection on the equatorial plane is the sun's declination. This formula calculates its value between +23.45 and −23.45 degrees.

$$\delta = -23.45\ \cos\left(\frac{360}{365}x(d+10)\right) \quad (5)$$

where α is the sun angle, which is the angle between the running beam and its projection on a horizontal surface, which can be calculated using the following equation [20]:

$$\alpha = 360/24 \times (T - 12) \quad (6)$$

$$T = \text{Local Time} + EOT - 4L_{local} + 60T_{zone} \quad (7)$$

$$EOT = -9.87\sin 2N + 7.53\cos N + 1.5\sin N \quad (8)$$

$$N = (360/364)\ x\ (d - 81) \quad (9)$$

where D is January 1's day of the week and T is Equality (7)'s time. Local Time is the standard local time in the affected time zone; EOT is the synchronized time to indicate the hub of the speed of the burgeoning revolution in the morning (minute); L_{local} is the local time; and T_{zone} is the different time zone relative to GMT (Greenwich Mean Time).

2.2. Fuel Cell

compared to the rate of hydrogen consumption (m_{H2}), PFC's output of the power is much higher:

$$P_{FC} = N \cdot I_{FC} \cdot E_{FC} \quad (10)$$

where N is the total number of cells and IFC is the current cell count [A]. EFC takes into account the electrical power required to heat a volume of cooking fuel (denoted by the symbol "V"), which is calculated as follows:

$$I_{FC} = \frac{2F}{N.\upsilon.M} m\dot{H}_2 \quad (11)$$

$$E_{FC}[V] = E_0 - b(\log(i)+3) - R_{ohmic} i - 0.000014e^{8i} \quad (12)$$

the constant F being Faraday's $[sA/mol]$; υ equation where M is the molecular mass of the reactant and A is the reaction area:

$$i = I/A \quad (13)$$

$$b = \frac{1}{2}\frac{\nu F}{RT} \quad (14)$$

The quantity of electrons transported, T, the fuel cell's operating temperature in degrees Celsius, and R are the gas constant in calories per mole of temperature-compressed gas. PEM fuel cells operate at 353.15 K (80 °C) to 393.15 K (120 °C). Open circuit voltage is $_{E0}$. Working cell temperature determines this number. The following formula calculates ohmic loss in E_q (13).

$$R_{ohmic} = r_m L_{mem} \quad (15)$$

where r_m refers to specific proton diffusion resistance (in centimetres) and L_{mem} is the permeability of a polymer membrane in centimetres. Table 3 shows the technical parameter input values for the computations.

Table 3. Main fuel cell simulation input data [21]

Paramètre	Symbol	Value
Température of opération (^oC)	T	80
The constant of Faraday $\left(\frac{sA}{mol}\right)$	F	96,485
Zone of Reaction (cm^2)	A	1000
Cell count (Σ)	n	82
Polymer membrane thickness (μm)	L_{mem}	125
Elemental resistance (Ω cm)	r_m	0.1
The ratio of reactants and products	υ	1

a voltage with no load (V)	E_0	1.17
Hydrogen's atomic weight $\left(\frac{g}{mol}\right)$	M	2

2.3. **Electrolyze**

A device that uses electricity to separate air into its component molecules, hydrogen and oxygen. Electricity consumption from electrolysers (ElecEL) is traced back to Qn-H2 and QH2 fuel cell functions. [22]:

$$Elec_{EL} = A_E Q_{n-H_2} + B_E Q_{H_2} \quad (16)$$

where AE = 15 (kWh/kg) and BE = 30 (kWh/kg) a Electricity consumption efficiency curve calculated using data [23]

2.4. **Hydrogen Tank**

The state of the hydrogen storage tanks is laid out in the next deal:

$$H_{2_{level}}(t) - H_{2_{level}}(t-1) = M_{H_{2-ele}}(t) + M_{H_{2-SCWG}}(t) - M_{H_{2-\tan k}}(t) \;/\; \eta_{H_2-\tan k} \quad (17)$$

where M_{H2-ele} and $M_{H2-SCWG}$ symbolizing the outflow of hydrogen from the petroleum and the steam-driven steam turbines. $\eta_{H2-\tan k}$ is the predetermined minimum efficiency of 75% for hydrogen fuel cells. Minimum Hydrogen Content in Tank H_{2-min} and maximum H_{2-max} set at a range between 5 and 90 percent, respectively.

2.5. **SCWG**

The following synthesis shows how the K-value model is used to determine species and abundance in response to gasification of supercritical biomass under certain conditions of temperature and pressure:

$$K_i = \prod_{j=1}^{N} a_j^{v_j} \quad (18)$$

Most of the biomass is agricultural waste and food scraps, with 40% water and a bulk composition of 48% carbon, 6% hydrogen, and 37% oxygen. SCWG reactors have simple reaction kinetics like this:

$$C_cH_xO_y + wH_2O \rightarrow x_1CO + x_2H_2 + x_3CO_2 + x_4H_2O + x_5CH_4 \quad (19)$$

where C, X, and Y represent biomass molecule components like glucose. w examines air mass release height during gasification. Carbon, hydrogen, and oxygen resource balances follow.

$$x1 + x3 + x5 - c = 0 \quad (20)$$
$$x + 2w - 2x2 - 2x4 - 4x5 = 0 \quad (21)$$
$$y + w - x1 - 2x3 - x4 = 0 \quad (22)$$

where x = 1–5 represents the zest's stoichiometric total. The concept of constant equilibrium, K, may reconcile two additional agreements to settle the aforementioned agreement system.

$$K_1 = \frac{x_{H_2} x_{CO_2}}{x_{H_2O} x_{CO}} \quad (23)$$

$$K_2 = \frac{x_{CH_4}}{(x_{H_2})^2} \quad (24)$$

The reaction temperatures determine the K_1 and K_2 values, which in the supercritical state may be expressed as follows [24]:

$$InK_1 = \frac{1674.732}{T} + (-4.721)InT + \frac{6.377*10^{-3}}{2}T + \frac{-1.952x10^{6}}{6}T^2 + \frac{0.641x10^{-5}}{2T^2} + 27.627 \quad (25)$$

$$InK_2 = \frac{6740.42}{T} + 1.622InT - 3.1\ x\ 10^{-4}T + \frac{31600}{T^2} - 9.504 \quad (26)$$

3. HRES Planning that Goes Beyond Economic Optimism

3.1. Optimization applied to a problem

If we desire efficient HRES, we must prioritize component size. An optimization model (Figure 1) is used to determine the appropriate HRES dimensions. The optimal size technique may be used with any HRES to maximize investment returns and system health. Optimization factors include HRES system processing power and storage. If demand is fulfilled, optimality may be determined by minimizing system costs or maximizing electricity profits. This paper presents the HRES power-generation mode optimization challenge.

3.1.1. Off-Grid Operating Mode

The best off-grid HRES design prioritizes cutting costs throughout the board:

$$Total\ Cost = \sum_i LCOE_i x E_i \quad (27)$$

Each component i (such as PV panels and biomass boilers) produces kilowatt-hours of power. HRES calculates LCOE as follows:

$$LCOE_i = \frac{\sum_{t=1}^{n} (I_{it} + M_{it})/(1+r)^t}{\sum_{t=1}^{n} E_{it}/(1+r)^t} \quad (28)$$

Where, I_{it} and M_{it} takes into account the costs of investing and operating each component *i* in year *t* system age indicator *n*.

3.1.2. Kisi Mode of Operation

The profit maximization challenge explains how solar panels may produce surplus electricity that can then be sold back to the grid. This surplus electricity can be defined as follows:

$$\text{Profit} = \alpha E_{dem} + \beta E_{sur} - \text{Total Cost} \quad (29)$$

E_{dem} is the amount of electricity needed in the selected residential area that is met by HRES (in kilowatt-hours); is the Feed-in-Tariff ($_{FiT}$) rate in Indonesia, which is equal to 28 IDR/kWh; and is the average price of electricity in Indonesia. Where E_{sur} is the additional electrical output (in kilowatt-hours) from PV panels.

3.2. Increased Requests

The primary objective in the first scenario (minimizing costs while maximizing profits) is to determine the best setup for the custom-designed system to meet the hourly electricity demand and supply in the residential zone of choice, taking into account the following caveats:

$$E_{FC}(h) + E_{PV}(h) = E_{dem}(h) \quad (30)$$

E_{pv} and E_{FC} consider the amount of electricity generated at each timestep h by the PV panels and the fuel cell, respectively.

3.3. Method of Solution

One met heuristic algorithm used to find approximate solutions to combinatorial optimization problems is the particle swarm optimization algorithm [25–29]. Because of communal organisms, an algorithmic issue occurs. Particles may travel with information transmission within the search space to find the optimum solution by using a search function as a target. This method, which consists of continuously searching for the best solution, uses a predetermined rate of acceleration for each iteration to propel the particle forward. The desired outcome is a swarm of cooperating particles that arrive at the optimal solution. The direction and speed of a particle's motion in all directions are determined by its vector. Each teammate's speed and positioning are updated in accordance with their own experience and the best articles from across the world. In order to get the best possible dimensions for the disassembled HRES's main components, PSO is used. The relationship between optimization and the simulated parts is shown in Figure 5. The simulation section may estimate daily hydrogen production and annual electricity generation given certain requirements for demand and environmental conditions (such as temperature and radiation levels). The PSO algorithm's fitness value is the sum of the individual HRES components' capacities, such as those of photovoltaic (PV) modules, fuel cells, electrolysers, hydrogen fuel cells, and steam-gas-water generators (SCWGs). To ensure that HRES satisfies annual electricity demand, the estimated value of suitability is tested using a simulation component. If the goal is not reached, the PSO algorithm will look for other values of fitness by changing the velocity and position of each particle using the aforementioned mixture:

$$v_{id}(t+1) = \omega \cdot v_{id}(t) + c_1 \cdot \varphi_1 \cdot (P_{id}(t) - x_{id}(t)) + c_2 \cdot \varphi_2 \cdot (g_{id}(t) - x_{id}(t)) \quad (31)$$

$$x_{id}(t+1) = x_{id}(t) + v_{id}(t+1) \quad (32)$$

4. Results and Discussions

4.1. Research the Crash Course

According to the regulations, HRES may be used in residential areas of the Tegal Island prefecture in Indonesia. A typical house in the residential area chosen in Figure 6 and its hourly ban rate. This diagram shows that the first ramp operates between 5:00 and 8:00 in the morning, when people typically begin their workday, and that the second ramp operates between 16:00 and 8:00 in the evening. When people go home after the day at night. In addition, winter months see much higher levels of electricity use due to the increased need for heating and lighting. A typical household's annual electricity consumption is predicted to be 4.37 MWh.

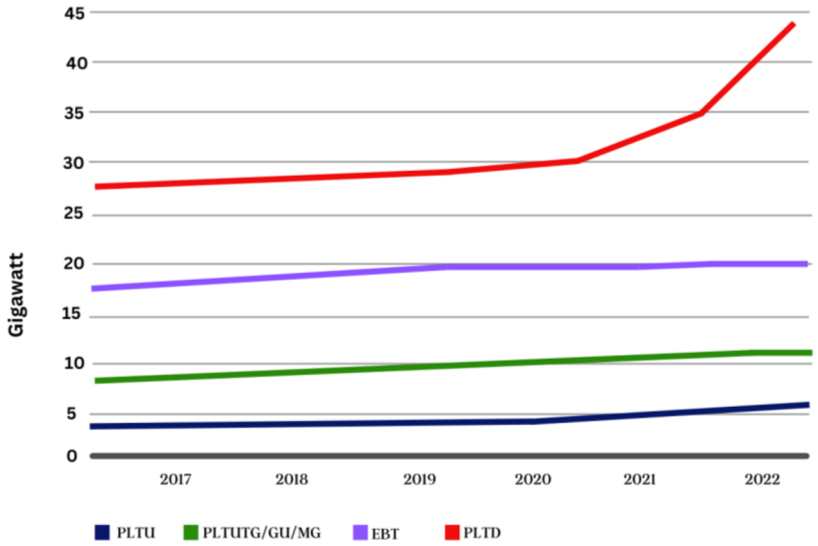

Figure 3. Installed Capacity of Indonesia's Power Plants by Type (2017-2022).

The average local temperature and global radiation dose at Tegal Island were compiled by the Indonesian Meteorological Agency (IMA) for the whole year of 2022, as shown in Figures 7 and 8. The peak months for worldwide broadcasting are April through June. In the month of August, worldwide radioactivity decreased somewhat. Since this region is affected by maritime winds, the state of the water varies greatly from summer to winter and spring to fall.

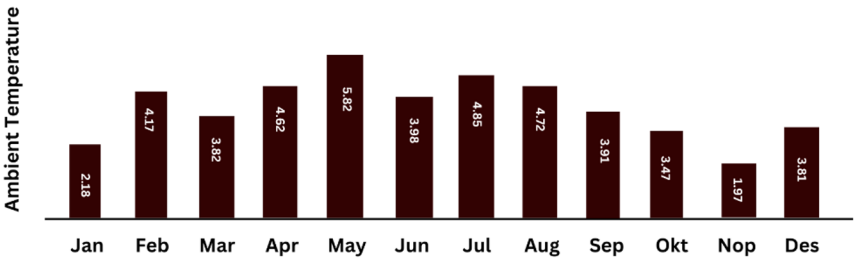

Figure 4. Tegal Island's average monthly temperature

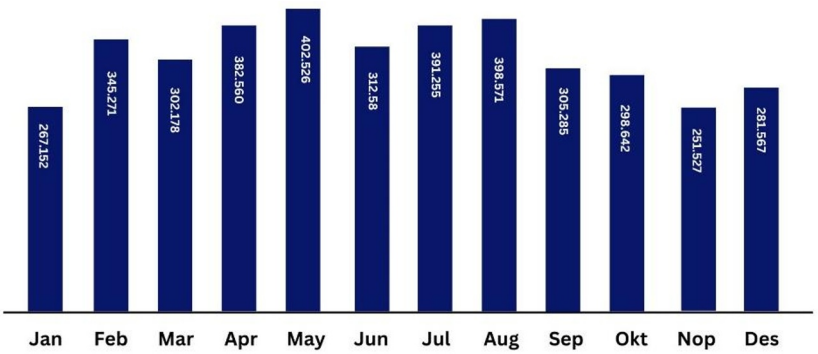

Figure 5. Average monthly solar radiation at Tegal Island.

4.2. HRES Cost Analysis

Module PV: Installation costs are estimated to be about 230 kW for residential rooftops, with annual maintenance costs estimated to amount to around 5% of the initial installation cost, based on a 20-year useful life [5, 30].

This 10-year research employed alkali electrolyze. An alkali air electrolyze costs 170 kW and 3 yen per watt to operate and maintain. BBQ fuel source installation costs 400 kW for 10 years. Operating and maintaining the PEM fuel delivery system costs around 1% of installation. Hydrogen storage tanks cost 150.000 kW for a 20-year lifespan and 9000 kW/year to operate and maintain.

Based on biomass feedstock processing capacity, SCWG reactors are priced. This research estimates daily feedstock costs of 42,000 kW per kilogram. [5]. SCWG estimates 610 kW hydrogen production costs. The cost of creating hydrogen via natural gas reformation, which averages 140 kW, is substantially lower.

4.3. Scenario Analysis

4.3.1. Scenario 1: Off-Grid Biomass-Powered System

Indonesian households squander around 6.46 billion tons of food annually. [31]. With 126,2 billion people in Indonesia in 2019, each person will generate 51,2 kg of food and fiber. Taking into account the assumption that there are four people living in each Indonesian home, the annual food waste generated by a single Indonesian family is estimated to be 204.70 kilograms (kg), making it suitable for use in the Sustainable Consumption and Production (SCPG) model. The results of this hypothetical are shown in Table 4. Solar photovoltaic panels (39%) and biomass fuel cells (61%) can meet the chosen residences' yearly power demands. Figure 6 shows hourly power usage under this scenario.

Due to the limited annual biomass supply in this scenario, the necessary hydrogen for providing cooking fuel must come from solar electricity generators. Increased demand for hydrogen for use in making cooking fuel during the colder months is largely attributable to the fact that less electricity is generated using solar power during the winter. This makes SCWG an important option for powering hydrogen generators. Since a single home can only produce a certain amount of wood over the course of a year, supplementary biomass sources like wood waste from nearby commercial buildings need to be taken into account. The average monthly electricity production from HRES assumed in this scenario is seen in Figure 10. The amount of electricity generated by burning biomass is higher in the winter than in other seasons. This is due to the fact that an excessive amount of electricity is required during the winter months, and the electricity generated by PV modules is insufficient due to inadequate sunlight. Monthly hydrogen production from a solar electrolyze and a steam-coupled water generator is shown in Figure 11.

Table 4. The idéal HRES configuration for Scenario 1.

PV Panel (kW)	FC (kW)	Electrolyze (kW)	Hydrogen Tank (kg)	SCWG (kg/h)
9	2.1	2.4	6	3z

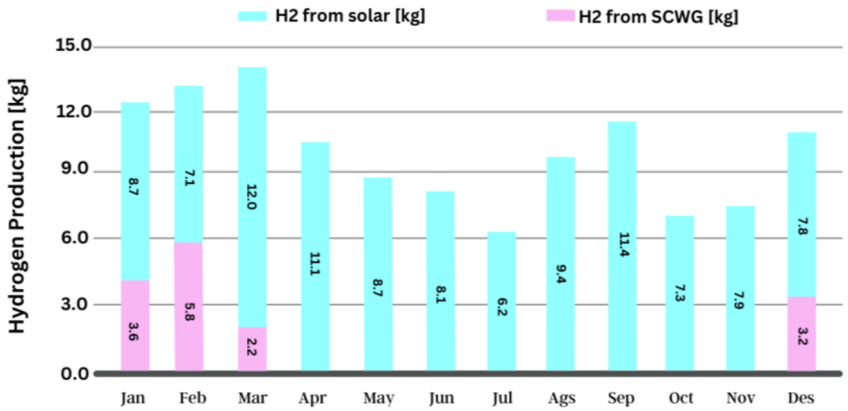

Figure 6. Monthly average hydrogen generation in scenario 1.

The optimal option costs 244,550 kW per year. This scenario has 55.92 IDR/kWh LCOE. Solar electrolysers now produce enough hydrogen for cooking fuel due to their increasing size. Figure 7 shows swarm behaviour during PSO iterations (0-20). Photovoltaic, fuel cell, and SCWG particles travel from their original conception to their optimum and global manifestations, converging at the ideal global position. Particles meet after 20 objective domain iterations between 0 and 5.

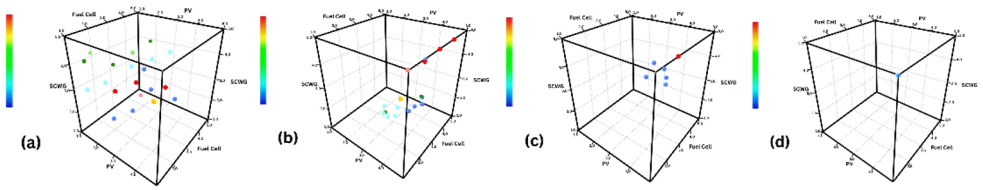

Figure 7. Particle position (photovoltaic vs. cooking ingredient vs. SCWG) for four distinct iterations: (a) = 0; (b) = 6; (c) = 18; (d) = 31

4.3.2. Scenario 2: Grid-Tied System Schema

In this scenario, HRES installation can generate total income in two ways: (1) by substituting HRES electricity for all electricity purchased to meet building demand, and (2) by selling back excess PV panel electricity to the grid at a profit, taking the feed-in tariff into account. Table 5 shows this scenario's optimum HRES settings. This model predicts 262,100 kW yearly system expenses. The predicted level zed cost of energy is 59.93 IDR/kWh, ensuring a clean profit of 15.140 for the system.

Table 5. Assumions Scenario 2, the best HRES configuration

PV Panel (kW)	FC (kW)	Electrolyze (kW)	Hydrogen Tank (kg)	SCWG (kg/h)
15	2.1	2.25	7.5	2

The size of the SCWG reactor and the PV panels will be increased to ensure that sufficient amounts of hydrogen are available for use in the production of fuel oil. In order to maximize profits, SCWG is first and foremost tasked with providing sufficient

hydrogen and filling up hydrogen pipelines. This will allow clean energy prices to rise when excess solar energy is sold back into the electrical grid. In this scenario, the maximum combined PV panel size for residential applications is 10 kW.

During the winter months, there is often a surplus of electricity of between 0 and 1 percent that may be used to offset higher electricity demand in the area's residential neighbourhoods. As a result of decreased electricity demand in the warmer months and transitional seasons, HRES will be able to inject a greater quantity of excess electricity into the grid.

Table 6 shows both scenarios' tekno-economic analysis model outcomes. Scenario 2 contrasts with Scenario 1 in that the PV module increases earnings by selling excess power to the grid. Scenario 1 has a lower projected LCOE than Scenario 2 when biomass feedstock is scarce, showing the value of cost reduction above profit maximization.

Table 6. The technical and economic analysis results for both possible futures.

Scenarios	Power Mix (%)		Annual Hydrogen Production Mix (%)		Annual Biomass Consumption (Kg)	Total Cost (IDR/Year)	LCOE (IDR/kWh)	LCOE, Including the annual Profit (IDR/Year)
	PV	PC	PV	SCWG				
Scenario 1	89	33	93	10	352.6	Rp.365,705	Rp.68.73	-
Scenario 2	92	30	93	10	352.6	Rp.372,420	Rp.71.54	Rp.86.77

5. Conclusion

We model and simulate hydrogen-based HRES to establish the ideal system design to suit Indonesian houses' power demands in Tegal Iland. Model development is optimized for cost and return. The simulation module estimates daily power production from the simulated HRES based on cooling and demand factors. The optimization model finds the system configuration that best meets demand while minimizing total system costs while operating off-grid and maximizing total profits from using cutting-edge electrical power and selling any excess to the grid. All scenarios reveal that the intended HRES can produce 47.3 MWh of energy, which is required to fulfill the study area's external demand. Scenario 1's system LCOE is 55.92 IDR/kWh, whereas Scenario 2's is 56.47. Scenario 2 has more electrolysis modules and photovoltaic cells utilizing biomass resources than Scenario 1. PV panel costs have increased while fossil fuel power plant prices have decreased due to biomass fuel shortages. The ideal profit maximization analysis shows that PV modules increase earnings by selling surplus power to the grid through the FiT mechanism. Under the greatest profit scenario with the FiT system, solar-hydrogen system cost reductions are critical. This research addresses HRES's greatest issues in residential buildings: cost efficiency and reduction. However, decision-makers who know the expenses frequently hesitate to invest in this sector. No major regulatory initiatives in Indonesia promote residential hybrid micro grids, despite local government incentives like feed-in-tariffs and J-Credits to compensate large-scale commercial and independent electricity generators' initial capital investments. Long-term policies and incentives to promote home micro grid deployment nationwide. This plan's demonstration program may assist governments set long-term objectives and prepare urban micro grids. This study provides cutting-edge technological information that may be used to create policies that provide hybrid micro grid owners with incentives or other assistance to optimize economic benefits to consumers, utilities, and society.

References

[1] Y. Sabri, H. S. Zein, and E. Yusuf, "Optimal cost valuation for renewable power plants using PSO in rural area," *Int. J. Electr. Eng. Informatics*, vol. 7, no. 4, pp. 613–629, 2015, doi: 10.15676/ijeei.2015.7.4.6.

[2] P. S. Pravin, Z. Luo, L. Li, and X. Wang, "Learning-based scheduling of industrial hybrid renewable energy systems," *Comput. Chem. Eng.*, vol. 159, 2022, doi: 10.1016/j.compchemeng.2022.107665.

[3] A. Singh, P. Baredar, and B. Gupta, "Techno-economic feasibility analysis of hydrogen fuel cell and solar photovoltaic hybrid renewable energy system for academic research building," *Energy Convers. Manag.*, vol. 145, pp. 398–414, 2017, doi: 10.1016/j.enconman.2017.05.014.

[4] H. Farzaneh, "Design of a hybrid renewable energy system based on supercritical water gasification of biomass for off-grid power supply in Fukushima," *Energies*, vol. 12, no. 14, 2019, doi: 10.3390/en12142709.

[5] N. Takatsu and H. Farzaneh, "Techno-economic analysis of a novel hydrogen-based hybrid renewable energy system for both grid-tied and off-grid power supply in Japan: The case of Fukushima prefecture," *Appl. Sci.*, vol. 10, no. 12, 2020, doi: 10.3390/APP10124061.

[6] S. Rehman, H. U. R. Habib, S. Wang, M. S. Buker, L. M. Alhems, and H. Z. Al Garni, "Optimal Design and Model Predictive Control of Standalone HRES: A Real Case Study for Residential Demand Side Management," *IEEE Access*, vol. 8, pp. 29767–29814, 2020, doi: 10.1109/ACCESS.2020.2972302.

[7] K. Murugaperumal and P. Ajay D Vimal Raj, "Feasibility design and techno-economic analysis of hybrid renewable energy system for rural electrification," *Sol. Energy*, vol. 188, pp. 1068–1083, 2019, doi: 10.1016/j.solener.2019.07.008.

[8] A. Tiwary, S. Spasova, and I. D. Williams, "A community-scale hybrid energy system integrating biomass for localised solid waste and renewable energy solution: Evaluations in UK and Bulgaria," *Renew. Energy*, vol. 139, pp. 960–967, 2019, doi: 10.1016/j.renene.2019.02.129.

[9] V. Mudgal *et al.*, "Optimization of a novel hybrid wind bio battery solar photovoltaic system integrated with phase change material," *Energies*, vol. 14, no. 19, 2021, doi: 10.3390/en14196373.

[10] H. Al-Najjar, H. J. El-Khozondar, C. Pfeifer, and R. Al Afif, "Hybrid grid-tie electrification analysis of bio-shared renewable energy systems for domestic application," *Sustain. Cities Soc.*, vol. 77, 2022, doi: 10.1016/j.scs.2021.103538.

[11] A. Dahdal, J. Truby, and H. Botosh, "Trade finance in Qatar: blockchain and economic diversification," *Law Financ. Mark. Rev.*, vol. 14, no. 4, pp. 223–236, 2020, doi: 10.1080/17521440.2020.1833431.

[12] B. Niu, F. Zeng, and Y. Liu, "Firms' introduction of internet-based installment: Incremental demand vs. cash opportunity cost," *Transp. Res. Part E Logist. Transp. Rev.*, vol. 152, p. 102277, 2021, doi: https://doi.org/10.1016/j.tre.2021.102277.

[13] M. Brolley and M. Zoican, "On-demand fast trading on decentralized exchanges," *Financ. Res. Lett.*, vol. 51, 2023, doi: 10.1016/j.frl.2022.103350.

[14] V. Subramanian, I. Vairavasundaram, and B. Aljafari, "Analysis of Optimal Load Management Using a Stand-Alone Hybrid AC/DC Microgrid System," *Int. Trans. Electr. Energy Syst.*, vol. 2023, 2023, doi: 10.1155/2023/7519436.

[15] Q. Tu, Z. Liu, B. Li, and J. Mo, "Achieving grid parity of offshore wind power in China–A comparative analysis among different provinces," *Comput. Ind. Eng.*, vol. 162, p. 107715, 2021, doi: https://doi.org/10.1016/j.cie.2021.107715.

[16] S. Praveenkumar *et al.*, "Techno-economic optimization of PV system for hydrogen production and electric vehicle charging stations under five different climatic conditions in India," *Int. J. Hydrogen Energy*, vol. 47, no. 90, pp. 38087–38105,

2022, doi: 10.1016/j.ijhydene.2022.09.015.
[17] A. A. DeFusco, H. Tang, and C. Yannelis, "Measuring the welfare cost of asymmetric information in consumer credit markets," *J. financ. econ.*, vol. 146, no. 3, pp. 821–840, 2022, doi: https://doi.org/10.1016/j.jfineco.2022.09.001.
[18] A. Shaqour, H. Farzaneh, Y. Yoshida, and T. Hinokuma, "Power control and simulation of a building integrated stand-alone hybrid PV-wind-battery system in Kasuga City, Japan," *Energy Reports*, vol. 6, pp. 1528–1544, 2020, doi: 10.1016/j.egyr.2020.06.003.
[19] M. F. Ishraque, S. A. Shezan, J. N. Nur, and M. S. Islam, "Optimal Sizing and Assessment of an Islanded Photovoltaic-Battery-Diesel Generator Microgrid Applicable to a Remote School of Bangladesh," *Eng. Reports*, vol. 3, no. 1, 2021, doi: 10.1002/eng2.12281.
[20] J. Feist and G. Feist, "ISE Theories of Personality," 2013.
[21] G. Jansen, Z. Dehouche, and H. Corrigan, "Cost-effective sizing of a hybrid Regenerative Hydrogen Fuel Cell energy storage system for remote & off-grid telecom towers," *Int. J. Hydrogen Energy*, vol. 46, no. 35, pp. 18153–18166, 2021, doi: 10.1016/j.ijhydene.2021.02.205.
[22] Z. Wang, X. Zhang, and A. Rezazadeh, "Hydrogen fuel and electricity generation from a new hybrid energy system based on wind and solar energies and alkaline fuel cell," *Energy Reports*, vol. 7, pp. 2594–2604, 2021, doi: 10.1016/j.egyr.2021.04.060.
[23] M. Dabirian, M. Kheradmandi, and M. Sedighizadeh, "Determination of the optimal capacity of electric hybrid renewable energy systems using a smart optimization algorithm," *IIOAB J.*, vol. 7, pp. 336–343, 2016, [Online]. Available: https://www.scopus.com/inward/record.uri?eid=2-s2.0-84997159390&partnerID=40&md5=a83e8a08ac0fa0817db226945b65236b
[24] S. A. Vaghefi, V. Muccione, R. Neukom, C. Huggel, and N. Salzmann, "Future trends in compound concurrent heat extremes in Swiss cities - An assessment considering deep uncertainty and climate adaptation options," *Weather Clim. Extrem.*, vol. 38, p. 100501, 2022, doi: https://doi.org/10.1016/j.wace.2022.100501.
[25] M. Shahvaroughi Farahani and S. H. Razavi Hajiagha, "Forecasting stock price using integrated artificial neural network and metaheuristic algorithms compared to time series models," *Soft Comput.*, vol. 25, no. 13, pp. 8483–8513, 2021, doi: 10.1007/s00500-021-05775-5.
[26] A. Fatih Güven and M. Mahmoud Samy, "Performance analysis of autonomous green energy system based on multi and hybrid metaheuristic optimization approaches," *Energy Convers. Manag.*, vol. 269, 2022, doi: 10.1016/j.enconman.2022.116058.
[27] S. Ajayan and A. Immanuel Selvakumar, "Metaheuristic optimization techniques to design solar-fuel cell-battery energy system for locomotives," *Int. J. Hydrogen Energy*, vol. 47, no. 3, pp. 1845–1862, 2022, doi: 10.1016/j.ijhydene.2021.10.130.
[28] R. Vatankhah Barenji, M. Ghadiri Nejad, and I. Asghari, "Optimally sized design of a wind/photovoltaic/fuel cell off-grid hybrid energy system by modified-gray wolf optimization algorithm," *Energy Environ.*, vol. 29, no. 6, pp. 1053–1070, 2018, doi: 10.1177/0958305X18768130.
[29] R. Hou, A. Maleki, and P. Li, "Design optimization and optimal power management of standalone solar-hydrogen system using a new metaheuristic algorithm," *J. Energy Storage*, vol. 55, 2022, doi: 10.1016/j.est.2022.105521.
[30] T. Hinokuma, H. Farzaneh, and A. Shaqour, "Techno-economic analysis of a fuzzy logic control based hybrid renewable energy system to power a university campus in Japan," *Energies*, vol. 14, no. 7, 2021, doi: 10.3390/en14071960.

[31] Suharyati and K. Utami, "Analysis of MSMEs Interest in Services Banking, Fintech and Cooperative," *Qual. - Access to Success*, vol. 23, no. 187, pp. 213–221, 2022, doi: 10.47750/QAS/23.187.27.